Journal of Alloys and Compounds 602 (2014) 8–15

Contents lists available at ScienceDirect

Journal of Alloys and Compounds

journal homepage: www.elsevier.com/locate/jalcom

Reduction synthesis of $Fe_xO_y@SiO_2$ core–shell nanostructure with enhanced microwave-absorption properties

Jing Zheng [a], Zongxue Yu [b], Guangbin Ji [a,*], Xiaohui Lin [a], Hualiang Lv [a], Youwei Du [c]

[a] Department of Applied Chemistry, College of Material Science and Technology, Nanjing University of Aeronautics and Astronautics, Nanjing 211100, PR China
[b] College of Chemistry and Chemical Engineering, Southwest Petroleum University, Chengdu 610500, PR China
[c] Laboratory of Solid State Microstructures, Nanjing University, Nanjing 210093, PR China

ARTICLE INFO

Article history:
Received 8 January 2014
Received in revised form 28 February 2014
Accepted 1 March 2014
Available online 12 March 2014

Keywords:
$Fe_xO_y@SiO_2$ core–shell nanostructure
Modified stöber method
Microwave-absorption properties
Hydrogen reduction

ABSTRACT

$Fe_3O_4@SiO_2$ core–shell nanostructures with different core diameter and shell thicknesses were prepared by modified stöber method and then converted into $Fe_xO_y@SiO_2$ by H_2. The structure, morphology and electromagnetic properties of $Fe_xO_y@SiO_2$ core–shell nanostructures were investigated. Experimental results demonstrate that the as-prepared $Fe_xO_y@SiO_2$ nanoparticles with deeply reduction not only exhibit significantly enhanced magnetic properties with maximum saturation magnetization values of 76.032 emu/g vs. 50.310 emu/g of $Fe_3O_4@SiO_2$ core–shell spheres, but also show enhanced microwave absorption properties with the maximum reflection loss value of −23 dB at 9.2 GHz under a thickness of 2.5 mm, which give forceful evidences that these $Fe_xO_y@SiO_2$ core–shell nanomaterials are attractive materials for microwave absorption applications.

1. Introduction

In recent years, electromagnetic interference (EMI) microwave absorption materials have already attracted extensive attention due to the expanded EMI problems, such as aircraft, biosensors, and medical devices [1,2]. The electromagnetic (EM) absorber is a kind of functional material which can effectively absorb EM waves, either by making EM waves loss through interference or convert EM energy into thermal energy. Nowadays, the way to design and synthesis the highly efficient microwave-absorbing materials with wide absorption frequency, high thermal stability and antioxidation have been intensively pursued due to their wide application. As we all know, magnetite materials with high values of magnetic permeability (μ) and dielectric permittivity (ε) are promising for EMI. As an important kind of functional magnetite materials, many works have been reported that Fe_3O_4 nanoparticles due to its amusing properties with the various structures [3–5] and the surface effect at high frequency, which effectively make the electromagnetic waves pass through owing to their high resistivity [6]. In addition, Fe_3O_4 has the characteristics of high magnetic permeability, saturation magnetization, favorable dispersibility and low cost, thus these advantages make Fe_3O_4 widely studied for microwave absorption absorbers [7–9].

However, Fe_3O_4 nanoparticles can be easily agglomerated to reducing the microwave-absorption properties. Moreover, Fe_3O_4 nanoparticles also have bad thermal stability which may be lead to lose single domain pole or special nature of magnetic materials, restricting the wide application for Fe_3O_4-based materials. Therefore, in order to synthesize Fe_3O_4-based magnetic nanomaterials with excellent microwave-absorption properties, different methods involving surface modification or a protective layer route with non-magnetic substances including SiO_2, TiO_2, Al_2O_3 have been developed [10]. These Fe_3O_4-based core–shell nanostructures, such as Fe_3O_4/Au [11], Fe_3O_4/SiO_2 [12], Fe_3O_4/TiO_2 [13], Fe_3O_4/C [14], have shown exciting magnetic properties. But there are still some problems, especially the low saturation magnetization and magnetic permeability which lead to the bad microwave absorption properties [15]. So how to upgrade the absorption efficiency of Fe_3O_4-based core–shell nanoparticles is still a challenge.

As far as we know, different microstructure of as-prepared samples can obviously influence their properties. The magnetic ferrites with hollow structure have some advantages, such as large specific area, low density and high mechanical stability [16,17]. Especially, the large pore volume in hollow composite spheres can act as a reservoir with a permeable barrier for controlling diffusion [18]. But for $Fe_xO_y@SiO_2$ core–shell nanomaterials, it is not sure that the above advantages can still exist after multi-step treatment. So its necessary to discuss the influence of the cores with solid and hollow structures on the microwave-absorption properties. In this

---

* Corresponding author. Tel.: +86 25 52112902; fax: +86 25 52112626.
E-mail address: gbji@nuaa.edu.cn (G. Ji).

http://dx.doi.org/10.1016/j.jallcom.2014.03.002
0925-8388/

paper, we reported a facile method to synthesize $Fe_3O_4@SiO_2$ core–shell nanostructure with solid and hollow core structures by covering a relatively stable SiO_2 layer on the surface of Fe_3O_4 nanoparticles. Importantly, ferromagnetic iron is an ideal candidate for microwave-absorption absorber due to its much higher magnetic permeability and more saturation magnetization (218 emu g^{-1}) when contrasted with Fe_3O_4. Therefore, the as-prepared $Fe_3O_4@SiO_2$ core–shell nanoparticles were converted into $Fe_xO_y@SiO_2$ under high temperature hydrogen reduction. Herein, various $Fe_xO_y@SiO_2$ core–shell nanoparticles with different core diameter and shell thicknesses have been successfully synthesized. After reduction, $Fe_xO_y@SiO_2$ nanoparticles were also kept well-defined in size and shape as the same with the $Fe_3O_4@SiO_2$ core–shell nanoparticles. The results show that $Fe_xO_y@SiO_2$ core–shell nanoparticles have significantly enhanced microwave absorption properties with the maximum reflection loss value of -23 dB at 9.2 GHz with a thickness of 2.5 mm, which strongly gives evidences that these $Fe_xO_y@SiO_2$ core–shell nanostructure materials are attractive materials for microwave absorption applications.

2. Experimental section

Synthesis of $Fe_3O_4@SiO_2$ nanoparticles

In a typical experiment, the started materials of solid (80 nm) and hollow Fe_3O_4 (340 nm) nanosphere were obtained by the method we reported previously [19]. And then $Fe_3O_4@SiO_2$ core–shell nanostructures were synthesized through a modified Stöber method. Specifically, specific amounts of Fe_3O_4 were pre-treated in hydrochloric acid solution (0.1 mol/L) with ultrasonic processing for 10 min to obtain the functional Fe_3O_4 nanoparticles, then dispersed them in a mixed solution of ethanol and water (a volume ratio of 4:1) and adjusted the pH value to about 10 by ammonia. Adding in drops of a certain amount of tetraethyl orthosilicate (TEOS) with continued stirring and aging for different times. After separating and drying the sediment, $Fe_3O_4@SiO_2$ nanoparticles were obtained. In addition, the thickness of silica shell can be controlled by changing the amount of TEOS and the time of hydrolysis.

Synthesis of $Fe_xO_y@SiO_2$ nanoparticles

The above-mentioned $Fe_3O_4@SiO_2$ particles with vacuum dry were annealed in a furnace at 723 K under a continuous hydrogen/nitrogen gas flow (with the flow of 1:1 volume ratio for H_2/N_2 atmosphere) for a certain time, and then cooled down to room temperature with a continuous H_2/N_2 gas flow to obtain the reduction samples of $Fe_xO_y@SiO_2$ core–shell nanoparticles. The schematic illustration of the formation process for $Fe_xO_y@SiO_2$ products as showed in Fig. 1. Particularly, the following Table 1 clearly demonstrates something about the as-synthesized $Fe_xO_y@SiO_2$ core–shell nanocomposites under different experimental conditions. Herein, the capital letters “C” and “R” stand for the coating and reduction steps, respectively; the letters of “a” and “d” represent the Fe_3O_4 hollow spheres (340 nm) and Fe_3O_4 solid nanospheres (80 nm), respectively.

Characterizations

The powder X-ray diffraction(XRD) patterns were recorded on Bruker D8 ADVANCE X-ray diffractometer using Cu Kα radiation ($\lambda = 0.154178$ nm) with 40 kV scanning voltage, 40 mA scanning current and scanning range from 10° to 90°. The field emission scanning electron microscopy (FE-SEM) images were obtained with the HITACHI S4800 type (after grinding the sample fully, then stick to conductive adhesive to take test). The transmission electron microscopy (TEM) images were taken on a JEOL JEM 2100 under a working voltage of 200 kV. The samples for TEM observations were created by dropping the ethanol suspension, containing the uniformly dispersed sample powders into carbon-coated copper grids. Fourier transform infrared spectrometer (FT-IR) were performed with Bruker Vertex 70 instrument operated at wave number range of 4000–400 cm^{-1} and KBr tabletting, in order to identify the chemical structure of functional group and determine type and structure of the compound. The magnetic performances (saturation magnetization and coercive force) were determined by a vibrating sample magnetometer (VSM, Lakeshore, Model 7400 series). The samples were mixed with paraffin wax in a certain mass fraction, pressing into the ring samples with the inner diameter of 3.04 mm and outside diameter of 7 mm in an abrasive medium. The electromagnetic properties (complex permittivity and complex magnetic permeability) of the samples were investigated using Agilent PNA N5224A vector network analyzer by the coaxial-line method.

3. Result and discussion

The SEM and TEM were executed to confirm the core–shell structure. When coating SiO_2 on the surface of Fe_3O_4, the time of hydrolysis and the amount of TEOS were both important factors. Fig. S1 showed typical SEM images of $Fe_3O_4@SiO_2$ nanoparticles with different hydrolysis time. As shown in Fig. S1(a), after 8 h of TEOS hydrolysis, the surface of the Fe_3O_4 nanoparticles was adhered with a small amount of SiO_2 particles. When the hydrolysis time was extended to 12 h (see Fig. S1(b)), we can find that a single independent microspheres without prior small particles were on the surface of Fe_3O_4 nanoparticles. It may be owned to the second-coated of originally attached SiO_2 particles on the surface of the composite particles by the way of dissolution and recrystallization process of SiO_2. From Fig. S1(c), we can see that the shell is composed of clustered SiO_2 nanoparticles on the surface, which has a tendency to increase with further extend the time of hydrolysis to 16 h. Therefore, the optical hydrolysis time to obtain as-prepared $Fe_3O_4@SiO_2$ nanocomposite with core–shell structure particles by modified Stöber method was chosen at 8 h or 12 h.

The amount of TEOS was another important factor. The $Fe_3O_4@SiO_2$ core–shell nanocomposites obtained with different amount of TEOS were investigated. Fig. S2(a and b) shows the SEM images of $Fe_3O_4@SiO_2$ composites with different dosage of TEOS. The appearance of the nanostructures shows that favorable monodispersity of ferric oxide nanoparticles are maintained in the composite material following with no reunion. Fig. S2(c and d) shows the TEM images of the $Fe_3O_4@SiO_2$ composite products with different dosage of TEOS. As has been extensively observed in Stöber processes, the product, which is obtained at 2.0 mL TEOS, contained shell-like particles with a thickness of less than 20 nm. When increasing the dosage of TEOS to 4.0 mL, the thickness of the shell composite particles was more than 20 nm which is not conducive to complete reduction under high temperature.

The XRD patterns of the samples before and after coating are shown in Fig. S3(a and b). The diffraction peaks at $2\theta = 30.16°$, 35.7°, 43.33°, 35.7°, 57.1° and 62.8° are corresponded to (220), (311), (400), (422), (511) and (440) of Fe_3O_4 crystal plane, respectively. After coating SiO_2, the peak intensity of Fe_3O_4 nanoparticles was little reduced and no obvious SiO_2 diffraction peak was found, suggesting that the SiO_2 existed as an amorphous state with low content.

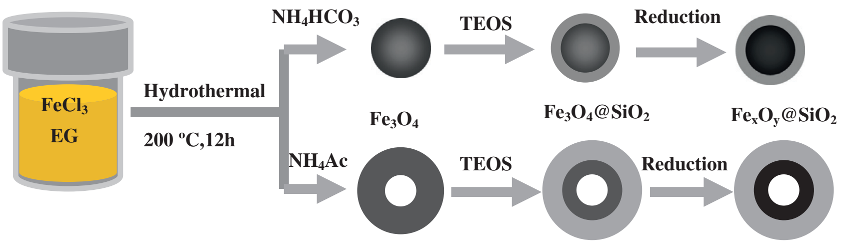

Fig. 1. Schematic path of as-synthesized samples.